Journal of Superconductivity and Novel Magnetism (2018) 31:3685–3689
https://doi.org/10.1007/s10948-018-4635-6

ORIGINAL PAPER

Enhanced Room-Temperature Ferromagnetism Observed in SiO_2-Coated CuO Nanostructures

Xiaofang Bian[1]

Received: 25 January 2018 / Accepted: 5 March 2018 / Published online: 13 March 2018

Abstract
In this paper, the magnetic properties of pure CuO and SiO_2-coated CuO nanocrystals were reported. Strongly enhanced room-temperature ferromagnetism was observed in SiO_2-coated CuO nanocrystals, whose saturation magnetization is two orders of magnitude enhanced compared to that of the uncoated CuO nanocrystals. The mechanism of this enhancement was investigated. It points out the main origin of ferromagnetism in these CuO nanocrystals is the uncompensated surface state, so that the coating of SiO_2 can effectively protect the surface state to improve the ferromagnetism in these CuO nanocrystals.

Keywords Nanocrystals · Copper oxide · Surface state · Ferromagnetism

Abbreviations

FM	Ferromagnetic
AFM	Antiferromagnetic
HMTA	Hexamethylenetetramine
XRD	X-ray diffraction
STEM	Scanning transmission electron microscopy
HRTEM	High-resolution transmission electron microscopy
FC	Field cooled
ZFC	Zero field cooled

1 Introduction

Semiconductors with ferromagnetic (FM) function are important in spintronics for injecting spins into nonmagnetic semiconductors in conventional spintronic devices, as well as for their applications in data storage and spin-valve systems. So many works are focused on the study of magnetic metal-doped semiconductors such as ZnSe, GaN, CeO_2, and ZnO [1–3]. Among them, CuO is a p-type semiconductor with a band gap of 1.2 eV, which has been widely applied in various devices, such as gas sensors [4, 5], catalysis [6, 7], field emitters [8, 9], electrochemical cells [10, 11], and magnetic storage media [12, 13]. CuO is also well known as a typical antiferromagnetic (AFM) material through their Cu–O–Cu superexchange interaction. When the sizes of CuO particles fall into nanoscale, the surface areas increase dramatically. The spins on the surface of such AFM nanostructures are actually not compensated, which are caused by mutually broken AFM sublattices [14]. These uncompensated surface spins lead to non-zero total magnetic moments which play a particularly important role for the vagaries of magnetic properties. As the size of the AFM nanostructures decreases, the surface spins may dominate the magnetism to exhibit visible FM properties in these AFM nanosystems. Several mechanisms have also been proposed to explain the FM properties in CuO nanostructures, such as intrinsic defects [15], vacancy [16], size effect [17], and the uncompensated surface state [18]. However, the main reasons inducing FM properties in pure CuO nanostructures remain controversial. Because of the enormous surface area, it is usually believed that the surface effect is dominated in these CuO nanostructures with FM properties [19, 20]. Actually, the surface states of these CuO nanostructures are inevitably affected by experimental treatment, such as drying. In most cases, these changes of the surface states will lead to the decrease of the surface spins, thus weakening the ferromagnetism of these CuO nanostructures. Therefore, it is expected that the ferromagnetism will be greatly enhanced if these surface spins could be effectively kept. However, as far as we know, such effort has not been reported yet.

✉ Xiaofang Bian
xiaofangbian@163.com

[1] College of Mechanical and Electrical Engineering, Shandong Management University, Jinan, 250357, People's Republic of China

In this work, we present the magnetic properties of CuO nanocrystals with frozen surface state by coating these nanocrystals with a thin shell of SiO_2. Enhanced room-temperature ferromagnetism was observed, while much weaker FM magnetization was found in the uncoated CuO nanocrystals synthesized by the same method. These results prove the significant surface effect on the FM properties of CuO nanocrystals.

2 Experimental Details

The CuO nanocrystals were synthesized by a microwave-assisted hydrothermal method. The raw material, a mixture of copper nitrate ($Cu(NO_3)_2 \cdot 3H_2O$, 25 mM) and equimolar hexamethylenetetramine (HMTA) solution was heated for 0.5 h with the power setting of 640 W. The precipitate was washed with deionized water several times and divided into three portions. The first portion of the as-grown collection was named as sample #1. The sample #1 was collected without any heat treatment so that it can not be detected by powder measurement. The second portion was dried at 60 °C in vacuum as sample #2. The CuO nanocrystals in the third portion were coated with a thin layer of SiO_2 ($CuO@SiO_2$) through a modified Stöber method with molar ratio of $CuO/SiO_2 = 5{:}1$ [21]. The coated CuO was dried at 60 °C in vacuum as sample #3. The samples were handled with extreme care during the whole sample preparation process to avoid spurious magnetic signals [22].

The structure, morphology and properties of these samples were investigated by x-ray diffraction (XRD, Philips), scanning electron microscopy (SEM, FEI Inspect F50), high-resolution scanning transmission electron microscopy (STEM, Tecnai G2 F20), and vibrating sample magnetometer (PPMS-9, Quantum Design).

3 Results and Discussion

Figure 1a presents the XRD spectra of pure CuO (sample #2) and $CuO@SiO_2$ nanocrystals (sample #3). Both samples are highly crystallized and the two curves have no obvious differences. All the diffraction peaks can be indexed to monoclinic phase CuO (JCPDS card 5-0661). SEM images of samples #2 and #3 are shown in Fig. 1b, c, respectively. The morphology of CuO nanocrystals has no obvious changes after being coated with a thin shell of SiO_2. Atomic ratio of Cu to Si was measured to be 5.33:1 by using EDX analysis (inset of Fig. 1c), which agrees well with the molar ratio of the reactants in the growth process.

Figure 2a is the TEM image of the as-grown CuO precipitate (sample #1) without drying. A leaf-like nanostructure

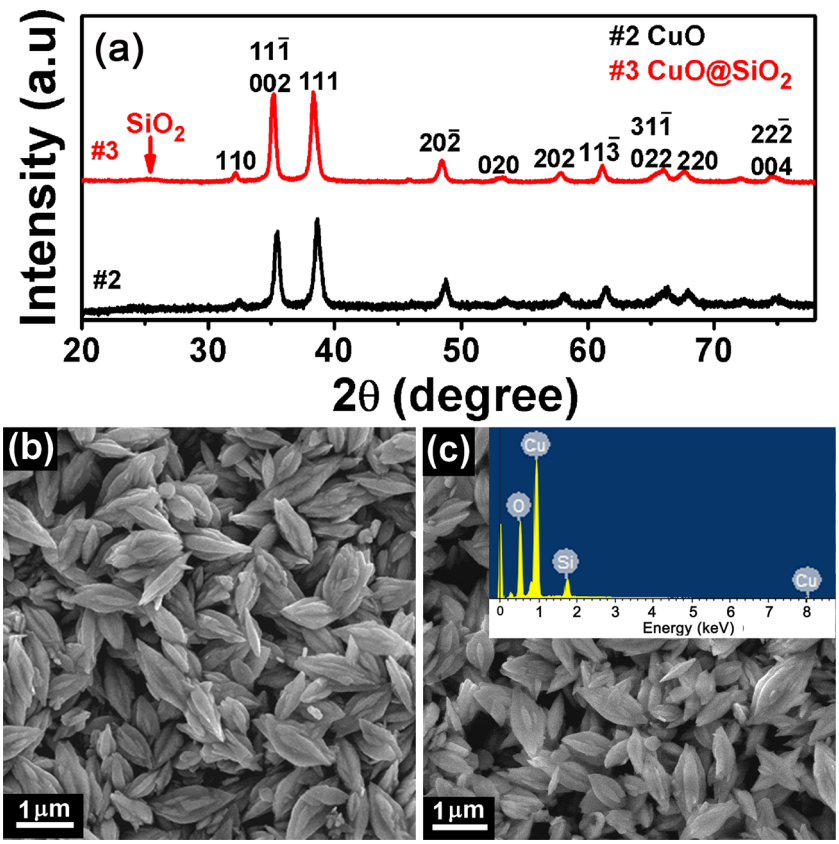

Fig. 1 **a** XRD spectra of pure CuO (sample #2) and $CuO@SiO_2$ nanocrystals (sample #3). SEM image of **b** sample #2 and **c** sample #3. Inset, EDX spectrum of sample #3

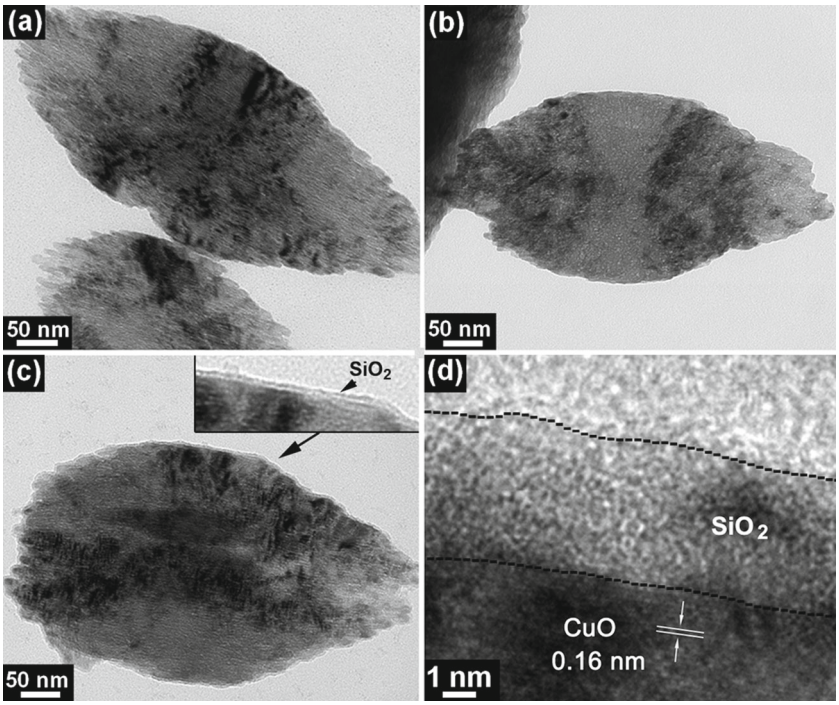

Fig. 2 TEM images of **a** as-grown CuO precipitate (sample #1), **b** dried CuO nanocrystals (sample #2), and **c** coated CuO nanocrystals (sample #3). **d** HRTEM image of sample #3

can be observed, with 500–600 nm in maximum diameter and 1–1.5 μm in length. It is noted that these nanoleafs consisted of a large number of tiny nanorods with diameter of $\sim$9 nm (Fig. 2a). A typical TEM image of the dried pure CuO nanocrystals (sample #2) is shown in Fig. 2b. However, no such tiny nanorod is found after drying treatment, as shown in Fig. 2b. This indicates that the sample is different from the products before drying. Figure 2c shows the TEM image of CuO@SiO_2 nanocrystals (sample #3). Large quantities of tiny nanorods also exist in the coated CuO nanocrystals and a thin layer of SiO_2 can be obviously observed in the locally magnified image (inset of Fig. 2c). Figure 2d shows the high-resolution transmission electron microscopy (HRTEM) image of a CuO nanocrystal surrounded by an amorphous SiO_2 shell. It is seen that the thickness of this SiO_2 shell is about 3.5 nm. As indicated in Fig. 2a–c, it can be concluded that drying treatment could do harm to these tiny nanorods but they are effectively protected after coating a shell of SiO_2. The shell of SiO_2 was not only coated on the surface of the whole nanoleaf but also deepened into the space between these tiny nanorods. As a result, this shell of SiO_2 can effectively protect the surface state of the samples by suppressing the fusion of these tiny nanorods.

The magnetization (M)-magnetic field (H) loops of the samples at 305 K are shown in Fig. 3. The CuO@SiO_2 nanocrystals (sample #3) have a much stronger magnetization than that of uncoated CuO (sample #2). The coercive force of sample #3 at 305 K is almost negligible, which is a typical characteristic of superparamagnetic materials. In the inset of Fig. 3, we have shown the magnetization versus temperature curves of sample #3 in zero field cooled (ZFC) and field cooled (FC) modes at 500 Oe external field. It indicates that the ZFC and FC curves of sample #3 start to split at 250 K and the divergence between the ZFC and FC magnetization curves increases with the temperature decrease. Such splitting phenomenon is similar to the feature of the spin-glass type behavior, which has been previously reported in CuO nanocrystals [23]. Furthermore, the maximum in the ZFC curve is located at 180 K, which is commonly ascribed to the average blocking temperature of the magnetic moments. The sample becomes superparamagnetic above this temperature, which is consistent with the behavior inferred from the hysteresis loops shown in Figs. 3 and 4.

Figure 4a plots the M-H loops of the samples at 10 K, while the enlarged M-H curve of pure CuO nanocrystals (sample #2) is shown in Fig. 4b. It is seen that the coercive forces of the samples can be clearly observed. The hysteresis loops indicate samples #2 and #3 exhibit both FM and AFM properties. The whole magnetization can be written as $M = MF + \chi H$, where MF represents FM term and the coefficient χ in the second term is the AFM and/or paramagnetic (PM) susceptibility. After deducting the contributions of PM and AFM signals, the saturation magnetization from the FM signal of sample #3 is measured to be 0.56 emu/g, which is two orders of magnitude stronger than that of sample #2. The two normalized curves of the FM signals are shown in Fig. 4c. It can be seen these two curves are overlapped closely.

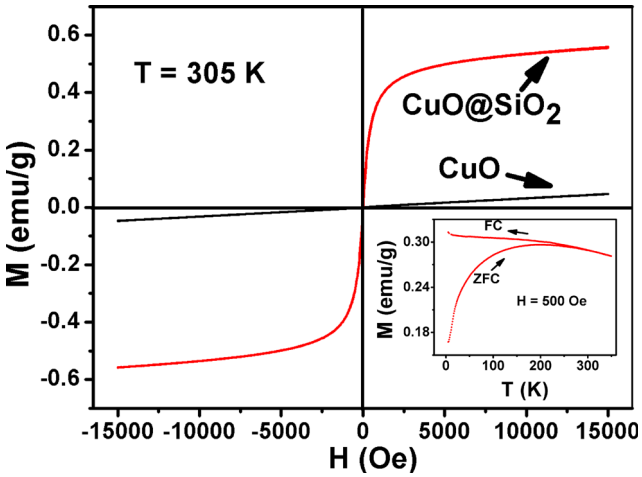

Fig. 3 Hysteresis loops for the samples at 305 K. Inset, temperature dependence of the magnetization for $CuO@SiO_2$

This shows that these two samples have proportionate FM properties, which probably result from the same FM origins. Since the shape of M-H curves is the characteristic of magnetic behavior, the overlapped curves may reveal that only simple enlargement of ferromagnetism is observed in $CuO@SiO_2$. The coercivities of samples #2 and #3 are measured being ~166 and ~241 Oe, respectively. The increase of coercivity in $CuO@SiO_2$ is a consequence of the change of the magnetic dipole coupling interaction after SiO_2 shell coating. By encapsulating on the particle surface, the SiO_2 shell decreases the magnetic dipole coupling interactions between neighboring nanoparticles. It is reported that strong dipole coupling interaction tends to assist magnetization reversal, thereby decreasing the coercivity [24, 25].

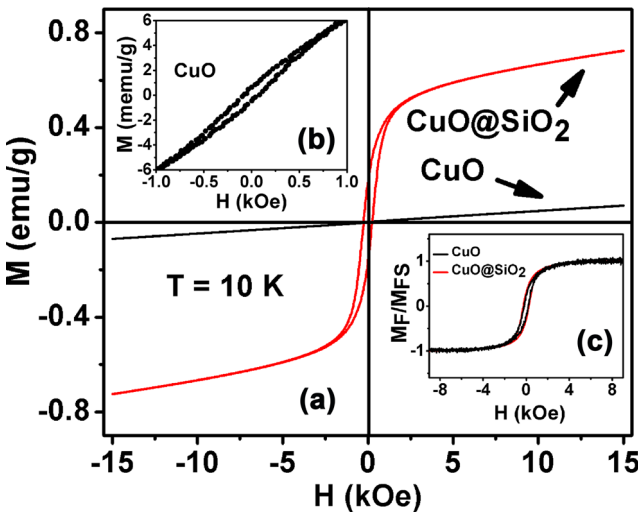

Fig. 4 **a** Hysteresis loops of the samples at 10 K. **b** Inset shows the enlarged central part of M-H curve of sample #2. **c** Inset shows the normalized FM curves of the samples

CuO is an AFM material through their Cu–O–Cu superexchange interaction. The surface of CuO nanostructures actually leads to a breaking of the sublattice pairing and thus produces uncompensated surface spins. So, FM properties are often observed in nanosized CuO and the magnetization is decided by the morphology. For example, Seehra et al. have reported CuO nanoparticles of 6.6 nm in diameter with a saturation FM magnetization ~0.008 emu/g at 5 K [26]. CuO nanorods of 30–40 nm in diameter were observed with a saturation FM magnetization ~0.05 emu/g at 305 K [27]. We note these CuO nanorods have rather strong FM magnetization, which may come from the fact that the rod shape reduces the surface coalescent during drying. In our work, it is obvious that the large enhancement of the ferromagnetism observed in $CuO@SiO_2$ origins from the change of the surface state due to the coating of SiO_2 for samples #2 and #3 have the same crystal structure and morphology. Thus, we hold that the uncompensated surface spins protected by the coating of SiO_2 dominate the measured magnetization. The SiO_2 shell can deepen into the space between the tiny nanorods to effectively protect the surface state of the samples to produce large FM magnetization. These well-ordered tiny nanorods also contribute to the enhancement of FM intensity through the interaction between them [28]. Therefore, a net increase of FM magnetization is observed in the coated sample, though SiO_2 is a non-FM material which may lead to the reduction of saturation magnetization for the increased mass of the nanocrystals associated with the silica shell. On the contrary, these uncompensated surface spins will be quenched along with the surface merge during drying, as shown in Fig. 2b. So, the remaining FM magnetization will be decreased. For those reasons, coating a thin layer of SiO_2 can effectively protect the surface state of CuO nanocrystals, so that rather larger magnetization can be obtained. This indicates that uncompensated surface spins play the leading role in producing enhanced magnetization in these CuO nanocrystals.

4 Conclusions

In summary, the enhanced room temperature ferromagnetism in $CuO@SiO_2$ nanocrystals is reported. It is found that the saturation magnetization of coated CuO nanocrystals is two orders of magnitude increased compared with the uncoated sample. This work points out that the coating of SiO_2 can effectually protect the uncompensated surface spins to produce large ferromagnetism, which may also applies to other antiferromagnetic nanomaterials such as NiO, CoO, MnO, and FeO.

Funding Information This work is supported by the Higher Educational Science and Technology Program of Shandong Province, China (Grant No. J16LJ02); Natural Science Foundation of Shandong Province, China (ZR2016GM26); and the Key Laboratory of Public Security Management Technology in Universities of Shandong (Shandong Management University).

References

1. Matsumoto, Y., Murakami, M., Shono, T., Hasegawa, T., Fukumura, T., Kawasaki, M., Ahmet, P., Chikyow, T., Koshihara, S., Koinuma, H.: Science **291**, 854 (2001)
2. Benstaali, W., Bentata, S., Abbad, A., Belaidi, A.: Mater. Sci. Semicond. Process. **16**, 231 (2013)
3. Liu, C., Yun, F., Morkoc, H.: J. Mater. Sci. - Mater. Electron. **16**, 555 (2005)
4. Zhang, J.T., Liu, J.F., Peng, Q., Wang, X., Li, Y.D.: Chem. Mater. **18**, 867 (2006)
5. Lupan, O., Cretu, V., Postica, V., Ababii, N., Polonskyi, O., Kaidas, V., Schut, F., Mishra, Y.K., Monaico, E., Tiginyanu, I.: Sensors Actuators B Chem. **224**, 434 (2016)
6. Sahay, R., Sundaramurthy, J., Suresh Kumar, P., Thavasi, V., Mhaisalkar, S.G., Ramakrishna, S.: J. Solid State Chem. **186**, 261 (2012)
7. Mendez-Medrano, M.G., Kowalska, E., Lehoux, A., Herissan, A., Ohtani, B., Bahena, D., Briois, V., Colbeau-Justin, C., Rodriguez-Lopez, J.L., Remita, H.: J. Phys. Chem. C **120**, 5134 (2016)
8. Hsieh, C.T., Chen, J.M., Lin, H.H., Shih, C.H.: Appl. Phys. Lett. **83**, 3383 (2003)
9. Zhan, R.Z., Chen, J., Deng, S.Z., Xu, N.S.: J. Vac. Sci. Technol. B **28**, 558 (2010)
10. Poizot, P., Laruelle, S., Grugeon, S., Dupont, L., Tarascon, J.M.: Nature (London) **407**, 496 (2000)
11. Moosavifard, S.E., El-Kady, M.F., Rahmanifar, M.S., Kaner, R.B., Mousavi, M.F.: ACS Appl. Mater. Interfaces **7**, 4851 (2015)
12. Díaz-Guerra, C., Vila, M., Piqueras, J.: Appl. Phys. Lett. **96**, 193105 (2010)
13. Raj, D.M.A., Raj, A.D., Irudayaraj, A.A.: J. Mater. Sci. - Mater. Electron. **25**, 1411 (2014)
14. Néel, L.: C. R. Acad. Sci. Paris **252**, 4075 (1961)
15. Muraleedharan, K., Subramaniam, C.K., Venkataramani, N., Gundu Rao, T.K., Srivastava, C.M., Sankaranarayan, V., Srinivasan, R.: Solid State Commun. **76**, 727 (1990)
16. Qin, H.W., Zhang, Z.L., Liu, X.Y., Zhang, J., Hu, J.F.: J. Magn. Magn. Mater. **322**, 1994 (2010)
17. Punnoose, A., Magnone, H., Seehra, M.S.: Phys. Rev. B **64**, 174420 (2001)
18. Kodama, R.H., Berkowitz, A.E.: Phys. Rev. B **59**, 6321 (1999)
19. Gao, D.Q., Yang, G.J., Li, J.Y., Zhang, J., Zhang, J.L., Xue, D.S.: J. Phys. Chem. C **114**, 18347 (2010)
20. Lu, P., Zhou, W., Li, Y., Wang, J.C., Wu, P.: Appl. Surf. Sci. **399**, 396 (2017)
21. Stöber, W., Fink, A., Bohn, E.: J. Colloid Interface Sci. **26**, 62 (1968)
22. García, M.A., Fernández Pinel, E., de la Venta, J., Quesada, A., Bouzas, V., Fernández, J.F., Romero, J.J., Martín González, M.S., Costa-Krämer, J.L.: J. Appl. Phys. **105**, 013925 (2009)
23. Narsinga Rao, G., Yao, Y.D., Chen, J.W.: IEEE Trans. Magn. **41**, 10 (2005)
24. Che, X.D., Bertram, H.N.: J. Magn. Magn. Mater. **116**, 121 (1992)
25. Du, H.F., Du, A.: Phys. Status Solidi B **244**, 1401 (2007)
26. Seehra, M.S., Punnoose, A.: Solid State Commun. **128**, 299 (2003)
27. Xiao, H.M., Zhu, L.P., Liu, X.M., Fu, S.Y.: Solid State Commun. **141**, 431 (2007)
28. Wu, M.Z., Xiong, Y., Jia, Y.S., Niu, H., Qi, H., Ye, J., Chen, Q.W.: Chem. Phys. Lett. **401**, 374 (2005)